WHITEPAPER

Thomas

The path to distributed hydraulic actuation

Model-based system design of enhanced mechatronic pilot systems

thomas-group.com

Michael Erhard
Sören Richter
Paul Roßmann
Martin Petzold

Thomas Magnete GmbH
Advanced Engineering
Innomotion Park 3
D-57562 Herdorf, Germany

unternehmenskommunikation@thomas-magnete.com

First publication within the 13th International Fluid Power Conference 2022 in Aachen from 13th to 15th June 2022.
Publisher: „Fördervereinigung Fluidtechnik e.V., Aachen“

Excavators creating a planum or digging a trench without an operator on the machine – are automated machine functions the near future? THOMAS can answer this not alone, but our products can pave the way. Modern mechatronic pilot systems for de-centralized axis control simplify interaction with the overall machine control by supporting the integration of assistance and automation systems. With the electro-hydraulic actuator, an intelligent and simple configurable component for closed-loop operation of directional control valves is available. Model-in-the-loop approaches lead to a robust and accurate controller design. Adaptation to different customer systems is taken into account both by the controller architecture and by supporting parameterization via self-adaptation. The integration of these functions thus maximizes customer benefits while leaving room for their own visions.

Keywords:
Control design, embedded electronics, model-in-the-loop

Target audience:
Mobile Hydraulics

1

Introduction

Introduction

1

Electrification in the construction and agricultural machinery sector has already led to the further use of electro-hydraulics for many years. The replacement of mechanical driven components with ones including proportional actuators such as solenoids or motors is not the only trend in this field of application. The integration of electronics improves product characteristics in terms of performance, efficiency and safety. Furthermore, the manufacturers' desire for machine-wide assistance and automation functions can also be realized with this type of products. The advantages are on the one hand the low cabling effort for necessary sensors and the achievable dynamics by avoiding signal transmission latencies. On the other hand, the machine control need not necessarily handle every single axis control. Thus, the implementation of machine-wide functions such as trajectory control including multiple axis benefits from this level of abstraction.

The electro-hydraulic actuator (EHA) shown in **Figure 1** is an innovative and configurable product made by THOMAS that enables the realization of machine-wide automation solutions. The EHA serves all customer requirements for controlling the aperture of directional control valves for mobile hydraulic axes. Exemplary fields of application include municipal vehicles, concrete pumps, cranes and tractors. Therefore, the EHA includes two proportional pressure-reducing valves, a redundant position sensor and an integrated electronic with field bus interface. With these properties, the EHA provides the link between the information processing and the power section of the machine. Adaption to different pressure and voltages levels is simply possible by changing the inserted pressure valves.

With such intelligent mechatronic devices as the EHA, the software with its features becomes the key component. Here, the software enables the implementation of various functionalities without having to change the hardware components. In addition, the integration and testing effort increases with these different features, moving efficient model-based development techniques such as model-in-the-loop to

1

the center of attention, especially in the development stage. Keeping this problem in mind, this article deals with the model-based design and testing of the entire control structure with the outlook on self-adaption to different customer systems. Especially in the case of de-centralized control, the exchange with the customer is a prerequisite for success. Therefore, the knowledge about the controlled system and its properties plays an important role during the design of the single software modules.

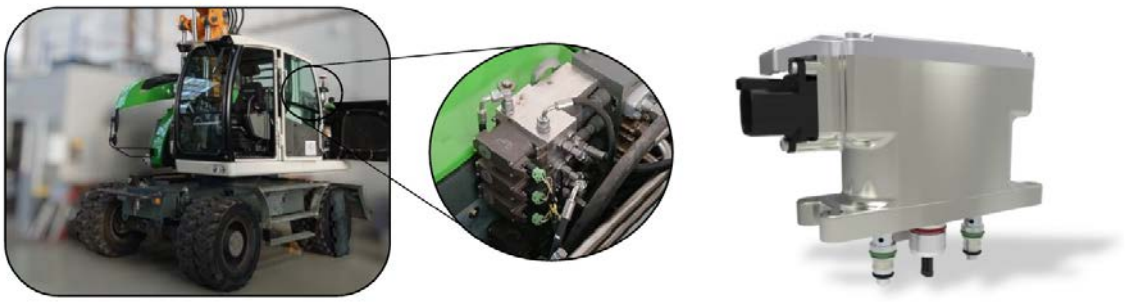

Figure 1: Electro-hydraulical actuator piloting directional control valves

This article is organized in the following manner: In the 2nd section the system of interest is analyzed whereas subsystems are defined for the model-in-the-loop (MIL) approach that follows. The first part of the 3rd section deals with the functional design of that part of the control structure originating from THOMAS as the supplier of the mechatronic pilot system. The customer system gets into focus in the second part. Here, a key challenge is the appropriate integration of the connected system with its often not fully known properties. The separate considerations end also in this section with the virtual pre-commissioning of the complete control structure. Based on the whole control design, discussions on self-adaption and its realization are held in the 4th section. The last section summarizes the content of this article.

System analysis

2

System analysis

2

The electro-hydraulic actuator shown in **Figure 1** drives the main spool in directional control valves used in mobile machines. A simplified illustration [1] of such a working section shows **Figure 2**. Here, each outlet port of the installed proportional pressure-reducing valves is connected to one side of the spool to be controlled. At the same time, an integrated spring presses the position sensor rod against the main valve spool making its motion with the embedded electronics detectable.

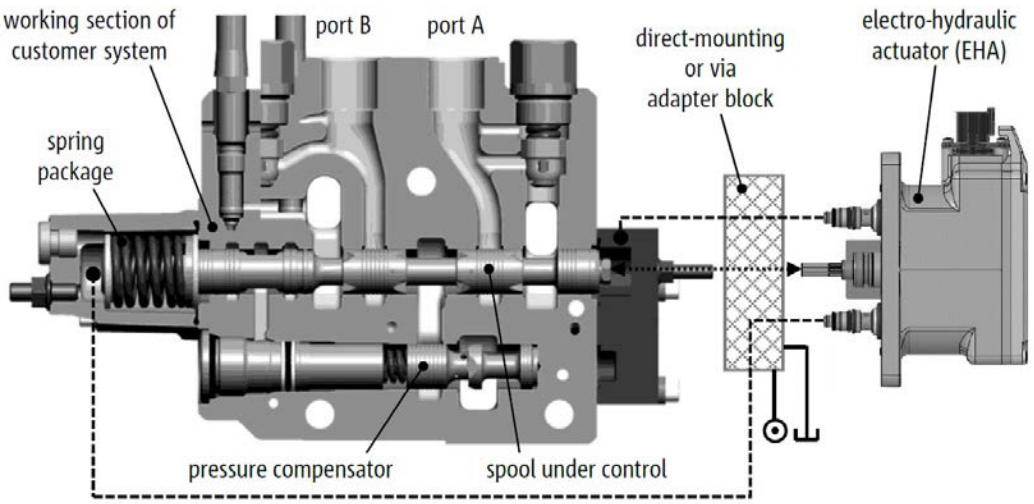

Figure 2: Exemplary customer system [1] with electro-hydraulic actuator (EHA)

The common principle of operation of the combined pilot-customer-system can be described as follows: with the energization of a solenoid, the corresponding pressure control valve causes a pressure build-up on one side of the valve spool inducing a pressure force on it. In open-loop mode, the spool position results from the balancing of the spring and pressure forces. Friction and flow forces act as disturbances on the force equilibrium causing position deviations depending on pressure and flow rate. A visual summary of these interdependencies is shown in **Figure 3**. Increased requirements for the accuracy of the controlled flow rates make it necessary to control the position of the main valve spool in closed-loop. From the pilot manufacturers' perspective, the interface to the customer system is the controlled pilot pressure p_{Outlet}. Although the pilot supplier can influence all elements up to this interface, the final performance is additionally influenced by system parameters of the

2

customers' system such as pilots' pump p_{Pump} or tank pressure p_{Tank} or interface reactions such as Q_{Outlet}.

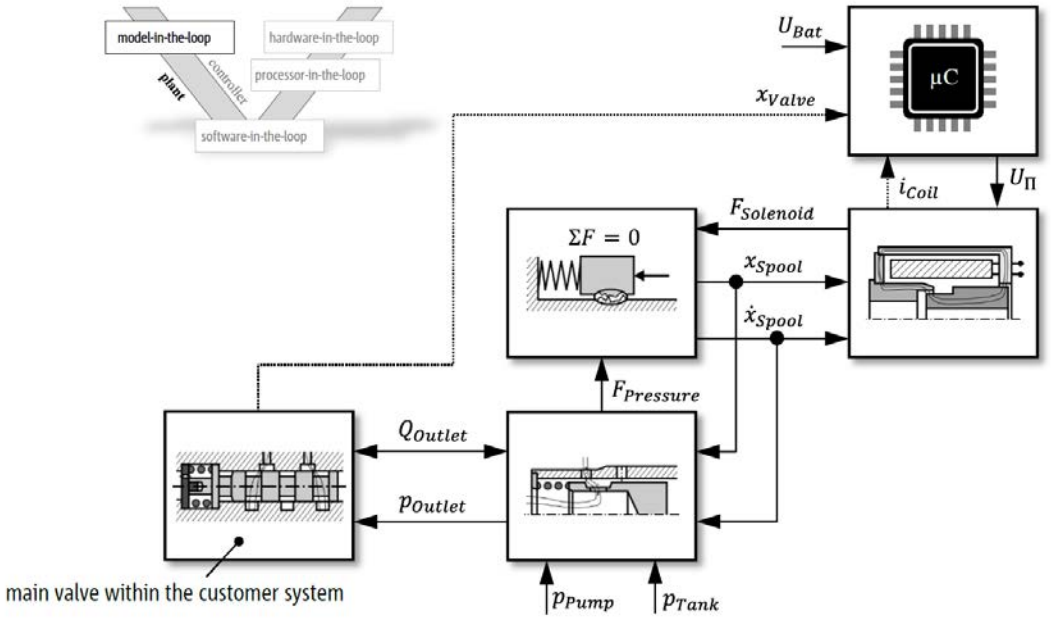

Figure 3: Simplified schematic representation of the physical interaction structure for a single pilot circuit

With regard to the desired closed-loop position control, at least the main valve position x_{Valve} has to be measured.For the intended setup of a compact, stand-alone component, the EHA is equipped with an onboard position sensor whose signal is fed back to the embedded electronics. Bringing the physical components from **Figure 3** in a block diagram and dividing the entire system into three major subsystems, an idea for a suitable control scheme is derived and outlined in **Figure 4**. In this illustration, the exchanged in- and outputs are the system states. A closer look also shows that these system states are relatively easy to measure and are thus available as a possible feedback signal.

Taking a closer look on the divided system from **Figure 4**, the clocked Voltage U_{Π}, adjustable by the micro-controller, is the system input whereas the valve position x_{Valve} is its output. Handling this system complexitywith only one control loop is not suitable due to the different time constants along the dependency path. For this reason and with the help of auxiliary control variables such as the coil current i_{Coil} or the

2

outlet pressure p_{Outlet}, an extended control loop is implemented. Hereby each downstream controller receives its setpoint from the output of the upstream loop – a well-known structure called cascade control. The exception for pilot hydraulics results from the structural setup of pressure-reducing valves as explained by Erhard [2]. Neglecting the spool dynamics inside these valves, the hydraulic-mechanical layout results in a proportional controller for an integral process. The vanishing errors for setpoint inputs and remaining deviations for disturbances are the typical properties of this structure apparent in each data sheet with characteristic curves for pressure-current and pressure-flow rate. For the sake of completeness, an additional pressure loop is outlined in parallel to the built-in functionality of the pilot valve.

The separation into individual control loops results in various advantages with regard to usability. In the case of open-loop operation, only individual blocks need to be switched off while the inner loops can continue to operate. Furthermore, the customer can limit himself to the parameterization that is relevant for him.

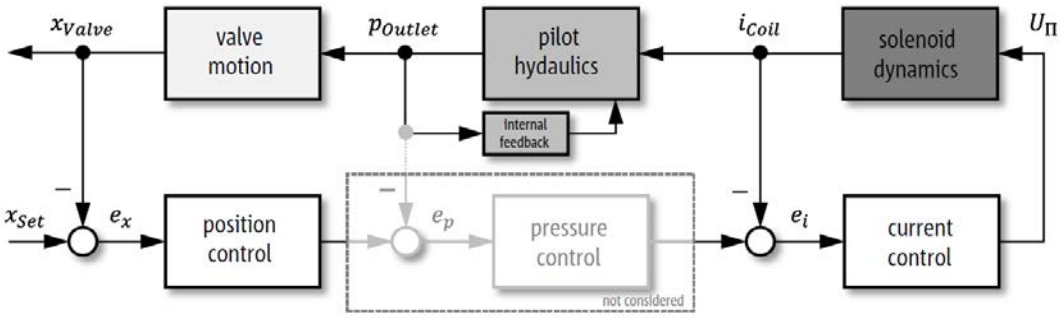

Figure 4: Cascaded position control layout for functional software design

Based on the chosen control structure form **Figure 4**, the following sections discuss the detailed control design, taking into account the subsystem specifics. Here, the relevant subsystem or the entire model serve as a virtual counterpart for the MIL approach. It is worth noting, that pilot valve design is not part of this article although its transfer function is an essential part of the entire feedback loop.

3

Model-based control design

Model-based control design

3

The cascaded control structure offers the possibility to design each controller in the feedback loop separately, starting with the innermost loop. According to Lunze [3], the inner loop acts as static gain if the cut-off frequency of the inner controller is significantly greater than that off the outer control loop. This condition should be fulfilled due to the strongly deviating time constants of coil inductivity and main valve movement. According to **Figure 4**, the starting point for the design process is the current controller described in the next section.

3.1 Current control loop

The design of the current controller aims to maximize the control performance independent of control strategies built into customer ECU's. Therefore, knowledge about the installed solenoids is used to robustly determine the controllers' parameters and completely de-couple the current controller from the customer. This is consistent with the objective of a stand-alone, automation-capable component.

Starting point for the model-based current control design is a nonlinear lumped-parameter simulation model for the solenoid including an eddy current diffusion network as well as motion induced effects. The model parameters for the considered solenoid come from data sheets or are computed with the finite-element-simulation.

3.1.1 System characterization

In a first step, results from this lumped model are used for static and dynamic characterization of the controlled system. Here the response of the solenoid is calculated for applied voltage ramps or steps. This gives enough information for fitting a linear time invariant transfer function $X_{Out}/X_{In}=i_{Coil}/U_{\Pi}$. **Figure 5** shows a summaryof the simulation results for static and dynamic inputs. It is worth mentioning that a nonlinear optimization technique with constraints is used to calculate the parameters of the chosen physical-based transfer function.

3

The results for the static gain from **Figure 5** are self-explanatory since the coil represents a constant resistance. Constant in this case means that there is no current-dependence of the resistor value or static gain K_S. Temperature effects caused by current-depending heating are neglected, but the robustness of the controller is verified for different resistance values. The results of the stair steps are much more interesting. For the nominal air gap of the solenoid, **Figure 5** clearly shows a non-negligible dependence of the time constant T_S on the average coil current i_{Coil}. Nevertheless, the transient response shows first-order-plus-dead-time (FOPDT) characteristics, an important property for the subsequent controller design.

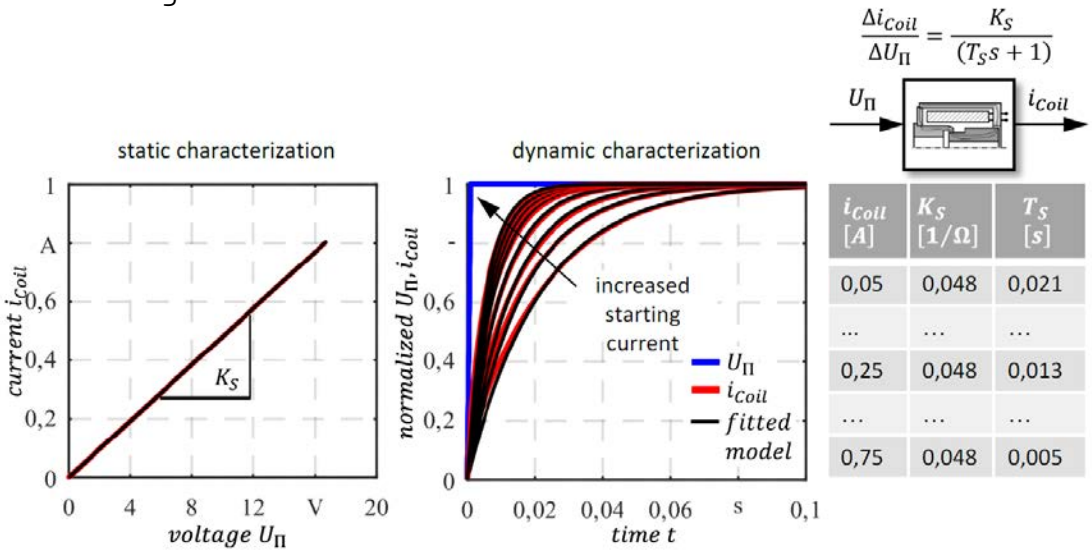

i_{Coil} [A]	K_S [1/Ω]	T_S [s]
0,05	0,048	0,021
...	...	...
0,25	0,048	0,013
...	...	...
0,75	0,048	0,005

Figure 5: Results of simulation-based solenoid characterization

Non-constant time characteristics complicate the design of linear controllers unless additional measures are considered. Taking into account the 4-times variation of the determined time constant, a consideration of this fact within the following design process is mandatory.

3

3.1.2 Control architecture

In advance, a decision must be made regarding the interaction of controller and power stage. Specifically, this involves the use of a switching controller directly driving a power source, or of a separate controller with its own dynamics in combination with a clocked power source. Advantage of the first one, the so-called hysteretic control, lies in its inherent stability as long as the controlled system is stable. In doing so, the response of the control loop is usually linked with the response of the system. With the well-known puls width modulation (PWM), a separate controller offers the possibility to shape the control behavior. Focusing on the last choice, the control design aims at a linear controller with additional measures dealing with existing nonlinearities, as outlined in **Figure 6.** The control architecture used is based on the state-of-the-art with a proportional part K_P and an integral part K_P/T_I connected in parallel. Nevertheless, the control architecture contains some important extensions.

First, detailed knowledge about the installed solenoid is used to compensate for the nonlinearity of the system, a well-known method called gain scheduling $K_P \neq const. = f(i_{Coil})$. At this point, the pilot valve supplier canbenefit from its component knowledge.

Second, the driving voltage U_Π for the solenoid is limited. In the case of unipolar excitation, the minimum level issimply represented by the off-state and the maximum level approximately by the supply voltage U_{Bat}. Innormalized notation, this corresponds to a duty cycle DC of 0 or 1. If the normalized output exceeds or falls below the previous mentioned limits then windup occurs in the integrator part of the control law. Compensation of these undesirable windup effects is often achieved by switching logic for the integrator part. However, a self-adjusting approach solves the problem in a better way. The so-called back calculation method mentioned by Visioli [4] uses the limit over- or underrun e_{DC} calculated with the saturated duty cycle DC_{Sat} in an additional feedback loop onlyfor the integrator part. This means that the difference between the unrestricted controller output and the saturation limits, scaled with a constant gain K_{Sat}, reduces the integral part so that no more limit violation occurs.

3

The only thing not handled until now is the negative influence of fluctuations in the power supply. This problem arises from normalizing the physical controller output to duty cycle with U_{norm}, as Equation (1) illustrates.

$$\frac{U_{\Pi}}{U_{norm}} = \frac{U_{Bat}}{U_{norm}} \cdot DC \tag{1}$$

If the normalization voltage differ from voltage supply, the solenoid receives a control signal that is too high or too low. The back-propagation of this influence into the control law indicates a scaling error in the control law.

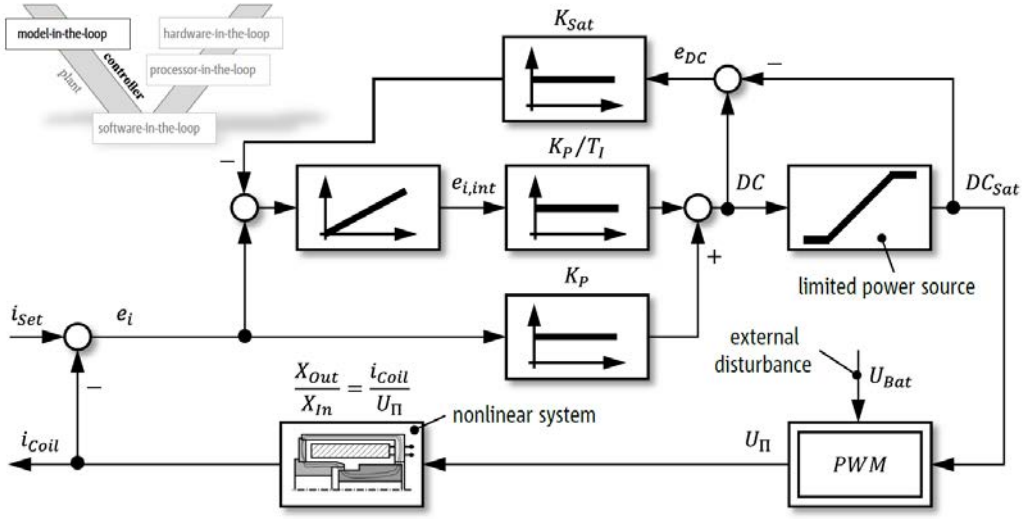

Figure 6: Extended PI-control architecture for current control loop

3

3.1.3 Model-in-the-loop testing and validation

The determination of the controller parameters is the last missing step before starting the tests. At this point, reference is made to the literature and the setting rules according to Chien, Hrones, Reswick for FOPDT-systems as printed by Zacher, Reuter in [5]. However, there is the difficulty of the non-existing dead time for the solenoid. Since ideal first-order transfer functions can be stimulated with extremely high proportional gains, the dead time of the PWM-frequency used later is considered. Based on the existing electronics and following [5], the PWM period T_{PWM} is chosen to allow quasi-continuous control also during digital implementation.

Figure 7 shows some simulation results for the solenoid and its current control. First, the controller is simulated continuously in time meaning that the output voltage is adjustable in each time step.

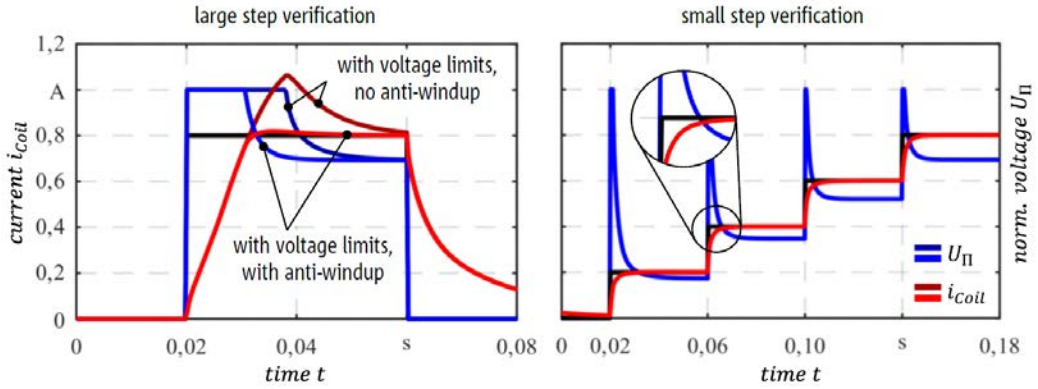

Figure 7: Continuous-time verification of anti-windup strategy and control accuracy/stability

Due to the limited voltage supply, the current rise time is limited in practice as expected. Even more dramatic appears the overshoot of the coil current successfully reduced by the anti-windup method applied. After considering the saturation-induced nonlinearity, the system nonlinearity and the associated gain scheduling come into focus. The results from **Figure 7** clearly show the successful handling of this system property recognizable by comparable small step responses. After this brief insight, the focus is now on the digital implementation of the control law, focusing on the characteristics of the microcontroller and its required peripherals.

3

The simplified block diagram of the corresponding discrete control law contains **Figure 8**. The main difference to **Figure 6** is the signal discretization resulting in additional dead times. Although the analog-to-digital conversion takes place with a multiple of the PWM period, the current averaging results in a dead time of half a period. Another dead time in the order of one period results from the finite calculation time of the microcontroller.

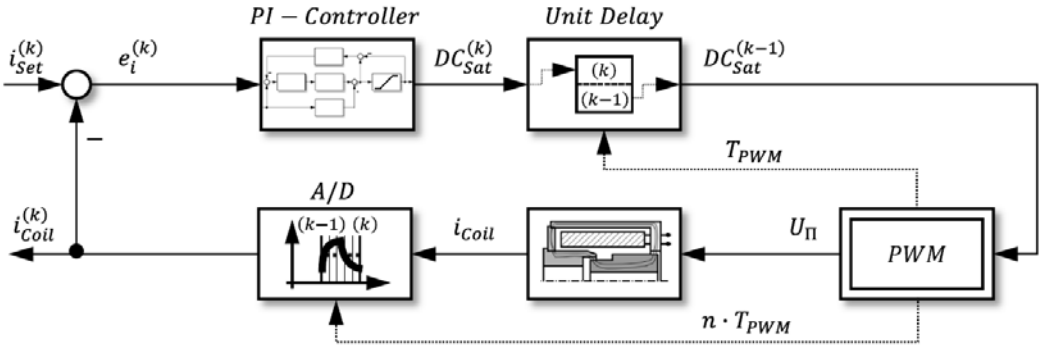

Figure 8: Discrete-time current control loop for digital implementation

So far, everything is in line with the state-of-the-art. To prevent further dead times and their influence on control stability, special attention must be paid to the algebraic loop in the anti-windup for the integrator, approximated with Euler-backward. In the saturation state of the controller output, only values of the current sampling time according to Equation (2) are used for the calculation of the new integral error $e_{i,int}^{(k)}$. The implementation of thistiming and calculation scheme on the microcontroller leads to the validation results shown in **Figure 9**.

$$e_{i,int}^{(k)} \cdot \left(1 + T_{PWM} \cdot K_{Sat} \frac{K_P}{T_I}\right) = e_{i,int}^{(k-1)} + T_{PWM} \cdot e_i^{(k)}[1 - K_{Sat} K_P] + T_{PWM} \cdot K_{Sat} \begin{Bmatrix} 0 \\ 1 \end{Bmatrix} \quad (2)$$

3

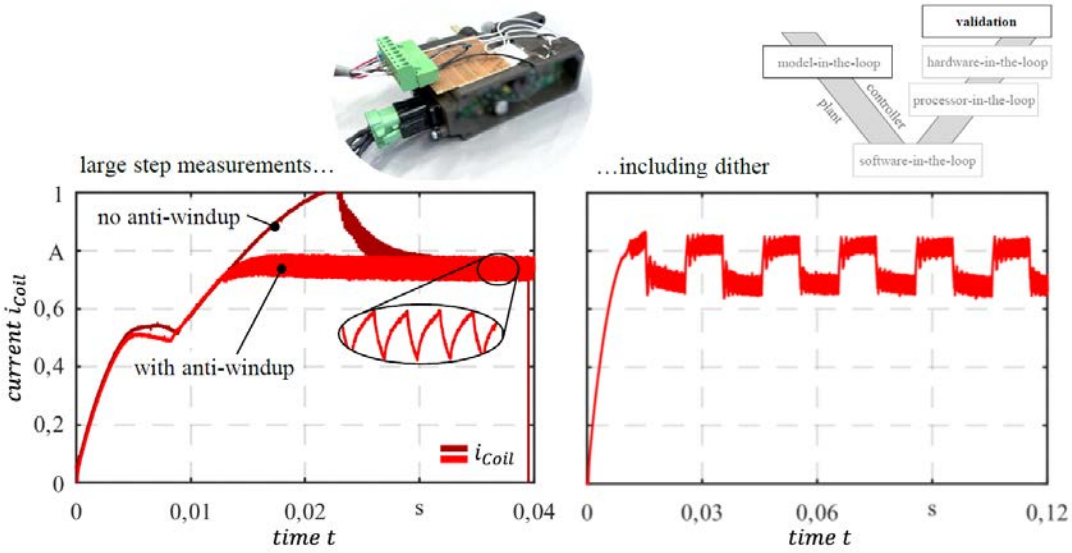

Figure 9: Discrete-time validation of dry solenoid (left) and in hydraulic operation (right)

Even if discrete-time simulation results are omitted in **Figure 9**, the validations impressively show the performance achieved. The control performance for large and small setpoint changes exhibits good dynamics and stability regardless of the step height. In both cases, with and without dither, accurate closed-loop control of an average current is easily possible. In combination with the chosen PWM frequency, the remaining current ripple is also acceptable. At this point, the model-based design, testing and validation of the inner current control loop is complete, and the focus must be placed on the outer position control loop.

3

3.2 Position control loop

The main difficulty in designing a suitable position control architecture is that the pilot valve supplier does often not know the customer system in detail. The generalized structure is to be selected so that different customer systems can be adequately controlled by parameter tuning alone. To ensure a high degree of usability and field customization, the number and complexity of the controller parameters shall be reduced to a level that can be handled practically. This necessarily leads to well-known, industrially widely used control structures.

Nevertheless, question arises as to which typical system responses the controller has to deal with. As a virtual reference serves again a lumped-parameter simulation model that could be parameterized with the help of one of our customers. However, it should be noted that this is just one example of the whole variety of customer systems available on the market.

3.2.1 System characterization

In accordance with section 3.1.1, the controlled system is excited with coil current ramps or steps to obtain and fit the underlying transfer function $X_{Out}/X_{In} = x_{Valve}/i_{Coil}$ of 3rd order modeling pressure build-up and valve motion. **Figure 10** shows the simulation and approximation results for the exemplary customer system selected.

3

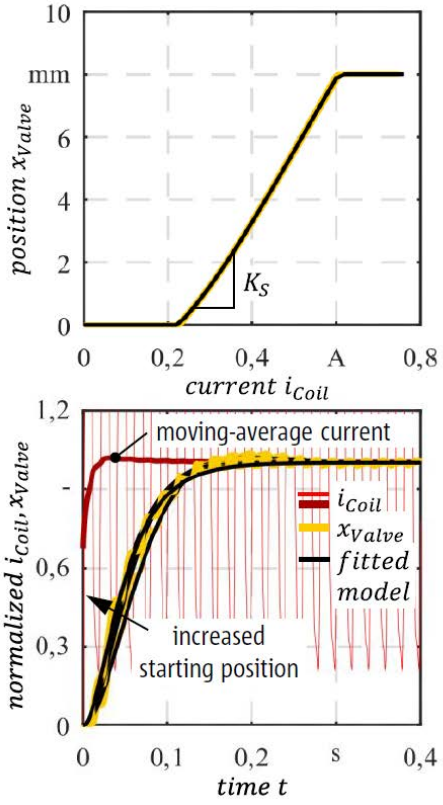

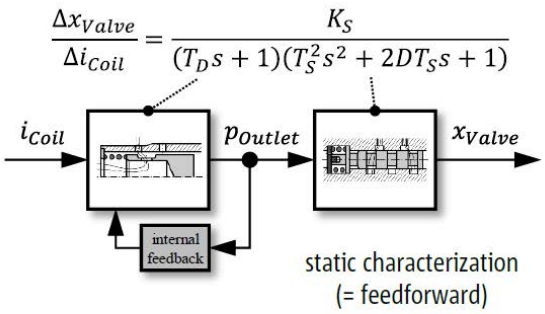

dynamic characterization

x_{Valve} [mm]	K_S [m/A]	T_G [s]	T_U [s]
2,5	0,021	0,074	0,010
3,7	0,022	0,072	0,009
5,1	0,023	0,071	0,008
6,5	0,023	0,072	0,008

Figure 10: Results of simulation-based customer system characterization

The determined static gain for the customer system under consideration has two nonlinearities, each localized in a subsystem, as shown in **Figure 10**. A fraction of the deadband in the current-position-response results from the pilot valve. The other fraction mainly originates from the spring preload on the main valve spool in the customer system. The saturation in the main valve position represents the end stop in one moving direction. The intermediate curve is weakly nonlinear and usually approximated by straight sections. The shape of the gain curve is similar across different customer systems as there are analogous physical interactions.

In contrast to the static identification, dynamic valve responses generally differ from one customer system to another. From a control-engineering point of view, the diameter of the main valve in combination with the spring package and the damping orifice between pilot valve and main valve spool are the most important factors influencing the natural frequency and the time response. Because of superimposed dither, the nor-

malized steps in **Figure 10** show a strongly fluctuating current putting the main valve into weak vibrations as well. The system under consideration show FOPDT-characteristic. For controller parameterization, not the individual values of the parameters within the fitted transfer function are of interest, but the variables derived from them. This includes both the dead times T_U and the compensation times T_G, whereby the ratio T_G/T_U indicates good controllability of the overall system. Here, the values are mostly constant in the operating range, but viscosity-related temperature effects can change them significantly.

3.2.2 Control architecture

As mentioned in the introductory part, usability plays an import rule in selecting a suitable control architecture. For this reason, and in accordance with the current controller, a modified PID-control law with anti-windup capabilities is chosen. Details about the continuous- and discrete-time realization were explained in the previous sections. Apart from the differential part of the control law, the only difference from the current control architecture is the possible use of a static feedforward current i_{FF}, as depicted in **Figure 11**.

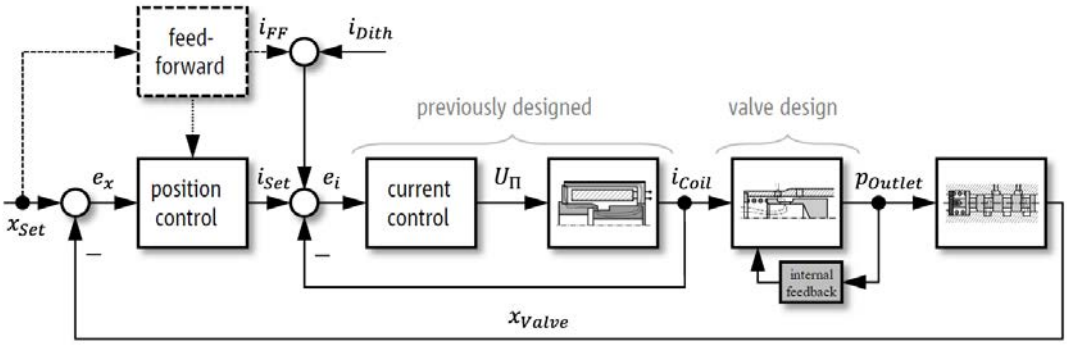

Figure 11: Complete cascaded control architecture for position control loop

Why static feedforward and closed-loop control in parallel? The exclusive consideration of the static part of the controlled system in the feedforward path is a consequence of the temperature-dependent side effects. A full model inversion can only consider one viscosity or temperature, so the other operating points are disregarded. Since the oil temperature in the pilot circuit is usually not known, static feedforward represents a

trade-off between accuracy and usability. If the feedforward path is not used, the position controller has a purely regulating effect, while the inclusion of the feedforward path in parallel to the feedback path improves tracking behavior.

The dither current i_{Dith}, also shown in **Figure 11**, adds the dither trajectory to the setpoint of the current controller.The location of the summation point between the cascaded controllers is necessary, because the dynamic properties of the position controller will otherwise distort the signal setpoint causing a reduced hysteresis minimization.

3.2.3 Model-in-the-loop testing and validation

In order to test the applicability of the selected structure together with der underlying customer system, controller parameters are predicted according to the setting rules for FOPD-characteristics with the objective of an asymptotic step response. Therefore, the corresponding times from **Figure 11** are used together with the inversion of the gain curve as model-based feedforward.

Starting point for the verification of selected and parameterized control architecture are the small and large step responses as shown in **Figure 12**. On the left side of this figure, the main valve follows the stepwise setpoint changes in comparable responses at each step. The only observable differences are in the first and last step. The dead times for the first step results from the summation of the individual fractions of pilot and main valve delaying the overall time response. In the last step, the main valve is pressed inside the end stop causing an abrupt stop of the movement.

3

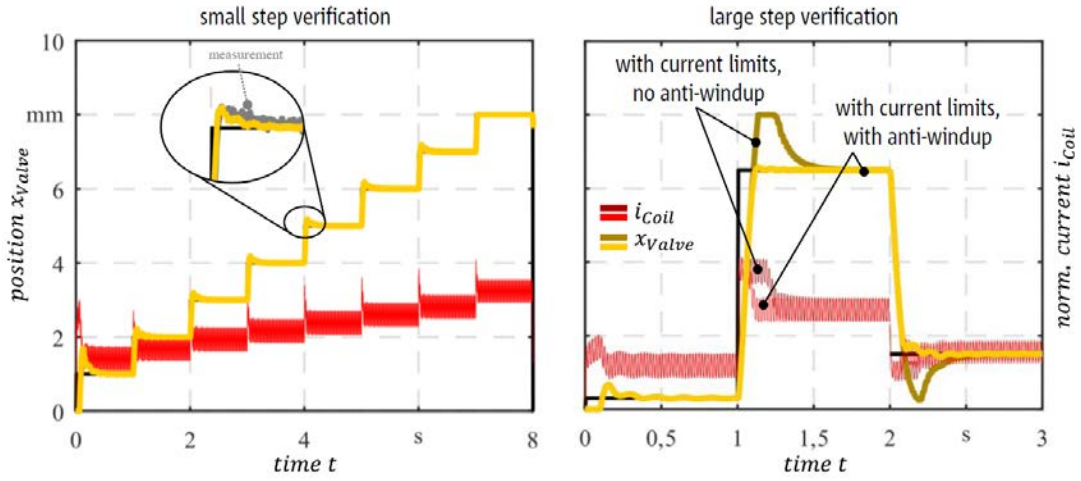

Figure 12: Continuous-time verification of control applicability and anti-windup strategy

In contrast to the expected behavior, the small step responses are characterized by a slight overshoot disappearing when the feedforward current is omitted. This difference results from the integrator part of the control law. In ideal PI-operation with vanishing steady-state error, the I-component generates the controller output alone. However, in simultaneous operation with the feedforward, this additional path takes over this part. Disappearing errors, however, require the sign of the error to be reversed, resulting in overshoot. A solution to this problem will discussed later in this section.

The large step shown on the right side of **Figure 12** indicates the same windup problem already known from the current controller. As a result of current limiting, large over- and undershoots occur. A special feature here, is that the lower limit corresponds approximately to the deadband current of the nonlinear gain curve. This prevents the controller output from entering a range without influence on the valve movement. Due to positive overlap, the actual minimum current setpoint in operation is usually higher than the deadband current. When anti-windup calculation is switched-on, the overshoots are similarly suppressed.

The transfer from a continuous-time approach to a sample-based implementation with its boundary conditions is less critical for position control than for current control. The inertia of the main valve causes a time response that is much slower than the current control period, so that the choice of the sampling frequency for the position control allows a lot of

3

flexibility. For the digital implementation and the validation measurements, a suitable integer divisor of the PWM frequency is used for each position control cycle.

The comparison of the step responses out of neutral position in simulation and measurement, as shown on the left side in **Figure 13**, dampens the positive overall impression. Although the initial dead times for different position commands are comparable, a large overshoot occurs in both simulation and measurement. This problem addresses a similar problem closely associated with the integrator part of the control law, the so-called deadtime windup. As long as the controller waits for a detectable change in position, the error remains constant causing an accumulation of the integral action over time. Commonly proposed methods such as de-tuning the controller parameters or having a dedicated deadtime for the integral path are suitable solutions, but reduce the dynamics and do not account for viscosity-induced deadtime changes. A more promising approach seems to be an intermittent integral action depending on the actual position error. By adapting the already existing anti-windup calculation scheme, an efficient numerical implementation is easily possible. The right side of **Figure 13** depicts the promising results. The additional measures reduce the deadtime-induced overshoot in both the simulation and the measurement. A positive side-effect lies in the likewise improved small step responses.

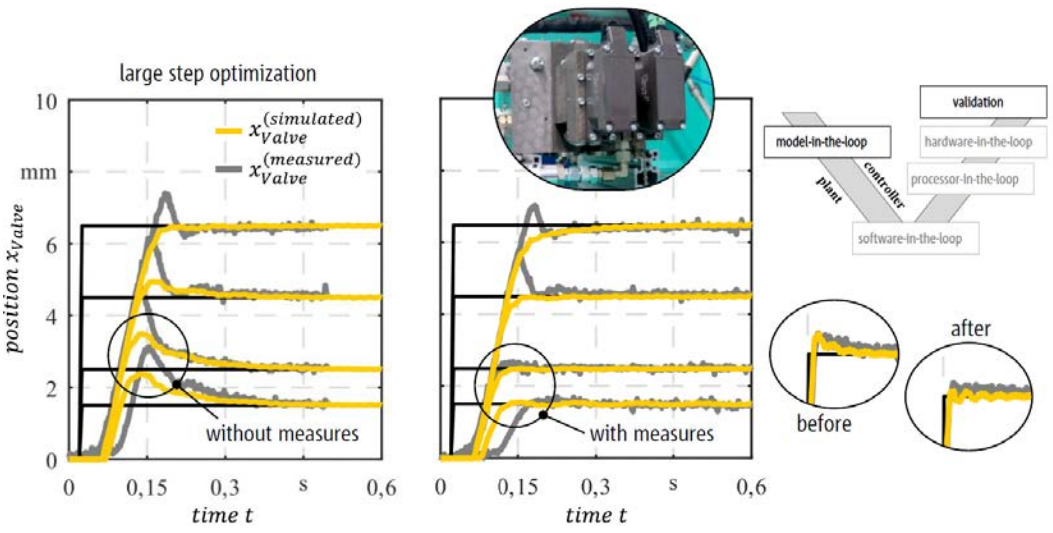

Figure 13: Discrete-time validation of cascaded control scheme with customer system connected

3

3.3 Summary

The model-based design of a cascaded control architecture was successfully completed focusing on easy and efficient reusability with respect to other valves or customer systems. The existing nonlinearities such as power limitation, spool overlap, spring preload and time delays from digital realization are handled appropriately in the control architecture or the controller parameters. The performance improvements achieved are not the only feature of this targeted approach. Individual steps inside this procedure can be the basis for the further development of innovative features such as self-adaption.

Self-adaption

4

Self-adaption

4

Only a brief insight into self-adaption to a customer system is possible in this section. As previously described, an initial determination of controller parameters based on standard rules is possible if system characteristics are known. This system identification is divided into a static and a dynamic characterization. For the identification to be online-capable, it's computational and data acquisition effort must be adapted to the microcontrollers' performance.

In this short section, the focus lies on the determination of the static gain curve additionally resulting in values for deadband current and maximum stroke. The idea behind the mathematical implementation is based on a recursive-least-squares optimization as explained by Schröder and Buss [6]. This approach avoids the need for gathering many data samples and standardizes the calculation effort. Equation (3) shows the numerical scheme for this method, using sorted dither-averaged measurements in our case.

$$\begin{aligned} \gamma^{(k)} &= \frac{P^{(k)}\xi^{(k+1)}}{1+\xi^{T(k+1)}P^{(k)}\xi^{(k+1)}}, \\ \theta^{(k+1)} &= \theta^{(k)} + \gamma^{(k)}\left(\psi^{(k+1)} - \xi^{T(k+1)}\theta^{(k)}\right), \\ P^{(k+1)} &= \left(I - \gamma^{(k)}\xi^{T(k+1)}\right)P^{(k)} \end{aligned} \tag{3}$$

The individual variables in Equation (3) are the target value ψ, the regressors ξ^T and the independent parameters θ.The matrix P is connected with the variance of the parameter vectors and updated every iteration. Using a convenient regressor formulation, interval-based learning of the static nonlinearity, as outlined in **Figure 14**, succeeds using a pre-defined steady-state excitation signal.

4

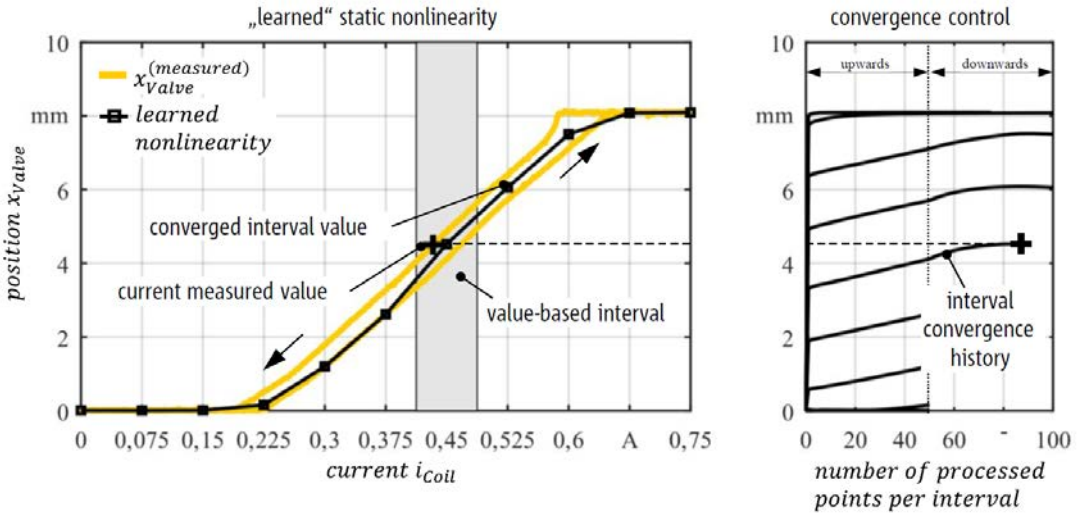

Figure 14: Learning results for static gain curve usable for self-adaption of controller parameters

Another advantage of this recursive approach is the easy monitoring of the convergence of the parameter values as outlined on the right side of **Figure 14**. Based on this curve, all required values for the control law are extracted or interpolated. The suitability of this approach for dynamic characterization is still under investigation and is outside the scope of this article.

Conclusion

5

Conclusion

In this article, the model-in-the-loop design stage as well as the validation stage of the cascaded control architecture used in intelligent pilot systems have been discussed. Particular attention was paid to the digital implementation of the current control law, including in-house expertise regarding the installed solenoid. This clearly demonstrates the advantage of modern embedded electronics in the realization of fast and accurate closed-loop controls. With constant consideration of user-friendliness, a successful design and parameterization of the position control loop essential for the customer took place. The selected control architecture supports the customer in customization and tuning of the control system and offers starting points for self-adaption. One of these points was briefly touched upon using the example of static feedforward identification. Another advantage of the model-based approach and the control laws used is the availability of tuning rules. With the help of these rules, online controller tuning is feasible without solving complex equations. The result of the adaption is only a reference value, but it provides the customer with a ready-to-use parameter set for his system in use.

Acknowledgements

6

Acknowledgements

This research and development project is funded by the German Federal Ministry of Education and Research (BMBF) within the collaborative project “Effizienz und Produktivitätssteigerung von Bauprozessen durch Vernetzung und Kommunikation mobiler Maschinen (Bauen 4.0)” (funding number 02P17D242). The author is responsible for the content of this publication.

Nomenclature & References

Nomenclature

Variable	Description	Unit
D	system damping coefficient	[-]
DC	duty cycle	[-]
DC_{sat}	saturated duty cycle	[-]
e_{DC}	duty cycle over-/underrun	[-]
e_i	current error	[A]
$e_{i,int}$	integral current error	[A·s]
e_p	pressure error	[Pa]
e_x	position error	[m]
$F_{Pressure}$	pressure force on valve spool	[N]
$F_{Solenoid}$	solenoid force	[N]
i_{Coil}	coil current	[A]
i_{Dith}	dither-related current	[A]
i_{FF}	feedforward current	[A]
i_{Set}	current setpoint	[A]
K_P	proportional gain	[...]
K_P/T_I	integral gain	[...]
K_S	system gain	[...]
K_{Sat}	saturation gain	[...]
p_{Outlet}	outlet pressure	[Pa]
p_{Pump}	pump pressure of pilot circuit	[Pa]
p_{Tank}	tank pressure of pilot circuit	[Pa]
Q_{Outlet}	outlet flow rate	[m³/s]
t	time	[s]
T_G	system compensation time	[s]
T_{PWM}	PWM period	[s]
T_S,T_D	system time constant(s)	[s]
T_U	system dead time	[s]
U_{Bat}	power supply voltage	[V]
U_Π	(clocked) voltage	[V]
x_{Set}	position setpoint	[m]
x_{Spool},$\dot{x}_{Spool}$	pilot spool position, velocity	[m, m/s]
x_{Valve}	main valve position (within customer system)	[m]

References

[1] **N., N.,**
K220LS – Mobile Directional Control Valve,
Catalogue HY17-8537/UK, Parker Hannifin Corporation, 2017.

[2] **Erhard, M.,**
Regelverhalten, Gestaltdesign und Robustheit direkt-gesteuerter Proportionaldruck-begrenzungsventile,
Dissertation, TU Dresden, Shaker Verlag, 2016.

[3] **Lunze, J.,**
Regelungstechnik 1: Systemtheoretische Grundlagen, Analyse und Entwurf einschleifiger Regelungen,
Springer Vieweg, Berlin, 2013.

[4] **Visioli, A.,**
Advances in Industrial Control: Practical PID Control,
Springer, London, 2006.

[5] **Zacher, S., Reuter, M.**
Regelungstechnik für Ingenieure: Analyse, Simulation und Entwurf von Regelkreisen,
Springer Vieweg, Wiesbaden, 2022.

[6] **Schröder, D., Buss, M.,**
Intelligente Verfahren: Identifikation und Regelung nichtlinearer Systeme,
Springer Vieweg, Berlin, 2017.

Thomas Magnete GmbH
Innomotion Park 3
57562 Herdorf
Tel. 02744 929-0
www.thomas-group.com